JOURNAL OF STRUCTURAL MONITORING AND BUILT ENVIRONMENT
e-ISSN: 2821-3432

JSMBE

Vol. 5 No. 2 (2025) 83-91
https://publisher.uthm.edu.my/ojs/index.php/jsmbe

Design and Tensile Performance of Face-to-Face Flange Connections of Cold-Formed Steel C-Section

S. N. A. Ismail[1], I. R. Muhammad Alif[1], A. F. Kamarudin[1]*

[1] *Faculty of Civil Engineering and Built Environment,*
Universiti Tun Hussein Onn Malaysia, 86400 Batu Pahat, Johor Darul Takzim, MALAYSIA

*Corresponding Author: fahmy@uthm.edu.my
DOI: https://doi.org/10.30880/jsmbe.2025.05.02.011

Article Info

Received: 5 September 2025
Accepted: 12 December 2025
Available online: 31 December 2025

Keywords

Cold-formed steel, face-to-face flange, shear performance, bearing performance, sleeve connection, Eurocode 3

Abstract

Cold-formed steel (CFS) is widely used in structural applications due to its high strength-to-weight ratio and material efficiency. However, the performance of its connections is often governed by localized resistance mechanisms. This study investigates the behaviour of face-to-face flange (FTFF) sleeve connections in CFS C-sections, with particular emphasis on bearing and shear resistances. Analytical design resistances were determined in accordance with Eurocode 3 (EC3), and experimental validation was conducted through laboratory testing of 9 specimens with varying plate thicknesses (0.75 mm and 1.00 mm), sleeve lap lengths of 200 mm, and screw quantities (4 and 6). Tensile test of the several types of connection styles was performed using a 120-ton universal testing machine. From the experimental results, it shows increases in material thickness and screw quantity primarily enhance connection performance through improved bearing resistance and load transfer efficiency. The ultimate tensile load (P_u) ranged from 15.20 kN to 29.21 kN. The calculated normalization ratios, defined as the ratio of the experimental load P_u to the design bearing resistance, exceeded unity and ranged from 1.27 to 1.67. This confirms that bearing deformation governed the failure mechanism. In contrast, the shear resistance ratios remained below unity, within a relatively narrow range of 0.54 to 0.85, indicating a significant margin, which is also influenced by variations in thickness and screw configurations. The failure modes were dominated by bearing deformation with hole elongation and localized plate yielding, accompanied by minor screw tilting, with no screw fracture observed. Finally, optimal FTFF connection performance can be achieved through a balanced design that enhances bearing and shear resistances by appropriately configuring material thickness and fastener number to improve connection capacity.

1. Introduction

Cold-formed steel (CFS) has emerged as widely utilized material in the construction industry due to its favorable structural and economic characteristics. Unlike hot-rolled steel, which is formed at elevated temperatures, CFS is manufactured through a cold-forming process at ambient temperatures, allowing for lightweight structural members with high strength-to-weight ratios. These properties make CFS a competitive option for both structural and non-structural applications, including roofing systems, wall studs, purlins, and composite flooring. In

construction practice, C-sections of CFS are commonly used in structural members such as purlins and side rails [1].

Despite its advantages, one of the most critical challenges in CFS structures lies in the reliability of its connections. Connection performance directly influences the integrity and safety of the overall structure. Due to thin-walled nature of CFS elements, connections are often more susceptible to local instabilities such as bearing deformation, tensile yielding, and screw shear-out, especially under tensile forces. In many cold-formed steel assemblies, self-drilling screws are commonly used as mechanical fasteners due to their ease of installation. However, these screw connections are prone to specific failure mods under axial loads, particularly when the connection detailing is insufficient or when the geometric parameters like edge distances and screw spacing are not optimized. One configuration that has drawn attention is the face-to-face flange (FTFF) sleeve connection. This setup involves overlapping flanges of two C-section, reinforced with a sleeve and fastened using multiple screws. While this configuration offers enhanced stiffness and is easy to fabricate, its structural performance under tensile loading remains inadequately understood. Factors such as thickness of the plate, lap length of the sleeve, and the number of screws play significant roles in determining the load transfer efficiency and failure mechanisms of the connection.

Several studies highlight how the thickness of the plate, sleeve lap length, and screw quantity influence connection behaviour. According to Wu et al. [2], the mechanical response of cold-formed steel joints depends heavily on screw patterns and material configuration. Roy et al. [3] reported that increasing screw numbers can enhance connection strength, although excessive screws may reduce efficiency per screw due to interaction effects. Similarly, LaBoube and Sokol [4] emphasized that flange thickness contributes to resistance against local failures such as bearing and tearing. Longer sleeve lap lengths improve load distribution and reduce stress concentrations near screw holes. Finally, according to Young and Chen [6], proper bolt spacing is critical in preventing premature shear failure in thin-walled cold-formed steel plates.

The current study addresses these gaps by focusing on FTFF sleeve connections subjected to tensile forces. The primary objective is to evaluate the shear and bearing resistance using Eurocode 3 (EC3) design provisions, and to verify these results through laboratory testing of tensile test. Specimens with varying geometries are analysed to understand how design variables influence ultimate strength and failure patterns. By correlating analytical predictions with experimental results, this study aims to offer practical recommendations for improving the design configuration of the CFS connections.

2. Methodology

The research employed three phases: analytical design experimental testing, and post-analysis.

2.1 Analytical Design

Design calculation followed Eurocode 3 [4], assessing shear resistance ($N_{v,Rd}$), and bearing resistance ($F_{b,Rd}$). Parameters included material yield strength (f_y), screw diameter, and effective cross-sectional areas.

2.1.1 Shear Resistance

According to Eurocode 3 (EN 1993-1-3), the shear resistance of self-drilling screws can be evaluated using Equation (1). The characteristic shear strength of the screw, denoted as Fv,Rk, is typically derived from the mill certificate provided by the manufacturer. In industry practice, 60 % of the minimum ultimate tensile strength is commonly used to estimate the shear strength of fasteners, particularly for single-shear joint design.

$$\mathrm{F}_{v,Rd} = \frac{F_{v,Rk}}{\gamma_{M2}} \tag{1}$$

$$\text{whereby, } \mathrm{F}_{v,Rk} = \frac{0.6 \times Pu_{screw} \times A_s}{\gamma_{M2}}$$

The A_s of M5.5 Hex self-drilling screw were calculated using Equation (2) based on ISO 898-1 and EN 1993-1-8 standard.

$$\mathrm{A}_s = \frac{\pi}{4}(d - 0.9382p)^2 \tag{2}$$

2.1.2 Bearing Resistance

In accordance with Eurocode 3 (EN 1993-1-3), the bearing resistance of a self-drilling screw is determined using Equation (3).

$$F_{b,Rd} = \frac{\alpha f_u dt}{\gamma_{M2}} \quad (3)$$

2.1.3 Calculations

Table 1 shows the sample of calculation for the bearing and shear resistances using equation (1) and (3). All parameter values used in these equations were obtained from the sample specifications, laboratory results, and mechanical properties (tensile strength of the screw and CFS plate) that derived from previous laboratory testing.

Table 1 *Analytical design resistances for shear and bearing*

Thickness (mm)	Bearing resistance (kN)	Shear resistance (kN)
0.75	$F_{b,Rd} = \frac{\alpha f_u dt}{\gamma_{M2}}$ $F_{b,Rd} = \frac{1.182(581.79)(5.50)(0.75)}{1.25}$ $F_{b,Rd} = 2.27\ kN$ per hole	$F_{v,Rd} = \frac{F_{v,Rk}}{\gamma_{M2}}$ $F_{v,Rk} = 0.6(f_u screw)(A_s)$ $= \frac{(60/100)(727.50)(16.34)}{1.25}$ $F_{v,Rd} = 5.71\ kN$ per screw
1.00	$F_{b,Rd} = \frac{\alpha f_u dt}{\gamma_{M2}}$ $F_{b,Rd} = \frac{1.364(636.27)(5.50)(1.0)}{1.25}$ $F_{b,Rd} = 3.82\ kN$ per hole	

2.2 Specimen Preparation

All design and detailing were verified according to the American Iron and Steel Institute (AISI 2016) [5] guidelines. The material properties, including yield strength and loading capacity of the CFS plates and fasteners, were first determined through laboratory testing and applied in specimen fabrication. A total of 9 specimens were prepared to reflect varying geometric and fastening parameters. The specimens differed based on plate thickness, sleeve lap length, and the number of screws. Two thicknesses were tested (0.75 mm and 1.00 mm), sleeve lap lengths of 200 mm were used, and each connection incorporated 4 and 6 self-drilling screws. Hex-head M5.5 self-drilling carbon steel screws, $^3/_4$ inch in length, were used as fasteners. Spacing and edge distances adhered to AISI minimums to ensure consistency with practical application. Specifically, screw spacing was maintained at 50 mm (≥ 3d), where d is the nominal screw diameter to prevent overlapping heads and strength reduction, edge distance was kept no less than 25 mm. The sample distribution of the laboratory samples is tabulated in Table 2.

Table 2 *Sample distribution and labelling*

No.	Thickness of CFS section (mm)	Sleeve Length (mm)	No. of screw	Specimen labelling
1	0.75	200	6	FTF1-C075-6-200, FTF2-C075-6-200, FTF3-C075-6-200
2	1.00			FTF1-C100-6-200, FTF2-C100-6-200, FTF3-C100-6-200
3	0.75		4	FTF1-C075-4-200, FTF2-C075-4-200, FTF3-C075-4-200

2.3 Testing Procedure

Tensile tests were conducted using a 120-ton Universal Testing Machine (UTM) following ASTM E8. The displacement-controlled setup ensured consistent loading rates. Each specimen's ultimate tensile load (P_u) was recorded, and failure modes were visually documented. The detailing of the FTFF sleeve connection and the illustration of testing setup is given in Figure 1.

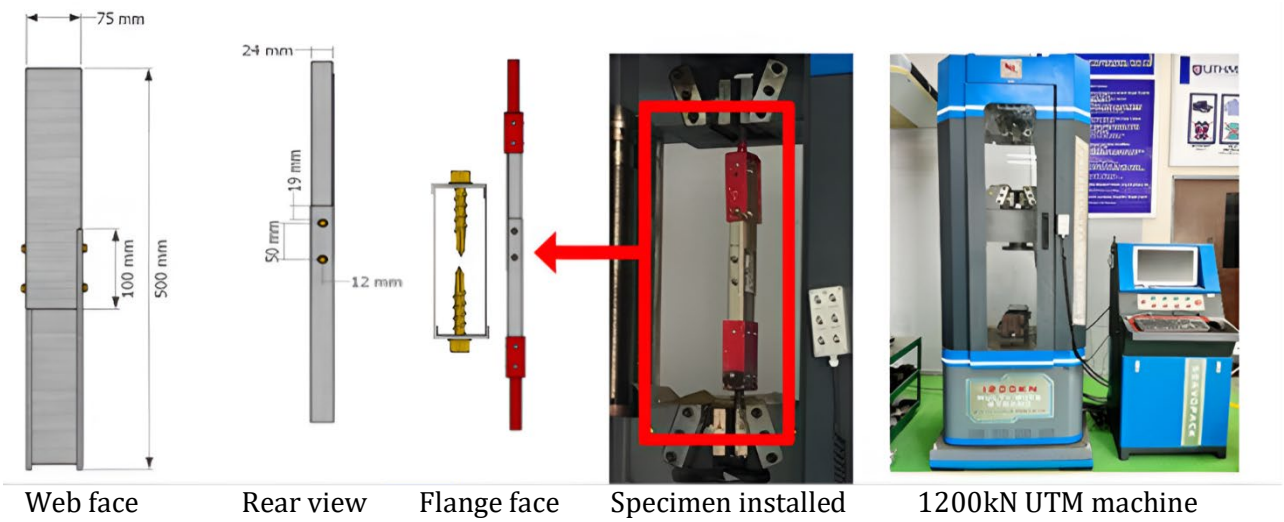

Fig. 1 *Schematic design of CFS connection and testing equipment for tensile tests*

3. Results and Discussions

This section presents the experimental results for CFS FTFF sleeve connections, compared against the design resistances from the analytical design calculation with the observed failure modes of the test specimens.

3.1 Ultimate Tensile Load

Table 3 shows the average ultimate tensile load (Avg. P_u) obtained from the peak values of the load–displacement curves from Figure 2 of the tested FTFF specimens. The results of two specimens (FTF2-C075-4-200 & FTF2-C100-6-200) were excluded due to irregular load–displacement behaviour, caused by the unexpected grip slippage of the jig during the testing. A clear trend can be observed, where specimens with greater material thickness and a higher number of screws achieved higher ultimate load capacities. The C100-6-200 specimen recorded the highest average ultimate load of 29.21 kN, reflecting the combined effect of increased plate thickness, and improved load distribution provided by the optimum number of fasteners. In contrast, the C075-4-200 specimen exhibited the lowest average ultimate load of 15.20 kN, which can be attributed to its thinner section and reduced fastener quantity.

Table 3 *Summary of Avg.* P_u

Specimen ID	Thickness (mm)	Sleeve Length (mm)	Screws	Avg. P_u (kN)	Comparison to the baseline sample
C075-6-200	0.75	200	6	23.10	+52 %
C100-6-200	1.00		6	29.21	+92 %
C075-4-200	0.75		4	15.20	Baseline (0 %)

The findings demonstrate that connection design parameters, including material thickness, number of fasteners, and sleeve length, are fundamental determinants of system performance. Examining the experimental data in Table 3 shows that when material thickness increased to 1.00 mm (with 6 screws maintained), ultimate load capacity improved up to 92 %. This improvement reflects the enhanced bearing resistance provided by thicker plate sections, which addresses the dominant failure mechanism in these connections. The results also highlight that fastener quantity influences performance more substantially than thickness alone. When the number of screws decreased from six to four in the 0.75 mm specimens, connection capacity declined by 52 %. This substantial reduction shows that adding screws from four to six meaningfully strengthens the connection by distributing loads more evenly among fasteners and minimizing stress concentrations at individual holes. Additionally, extended sleeve lap length promoted better force distribution throughout the connection, which delayed localized deformation and raised the ultimate load threshold. These observations establish that both geometric parameters and fastener layout are essential factors controlling the load capacities on shear and bearing performance of FTFF connections, as Table 3 illustrates.

J. of Structural Monitoring and Built Environment Vol. 5 No. 2 (2025) p. 83-91

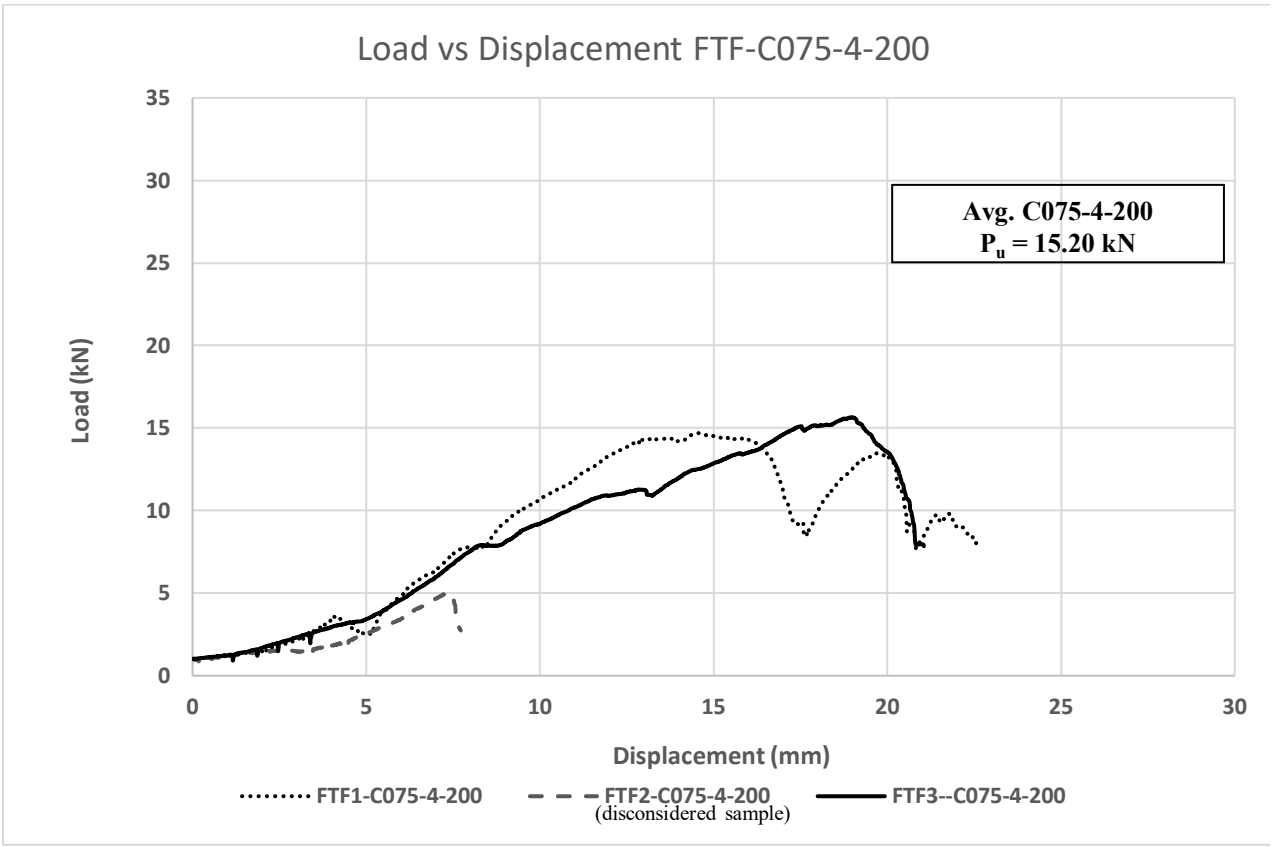

(a)

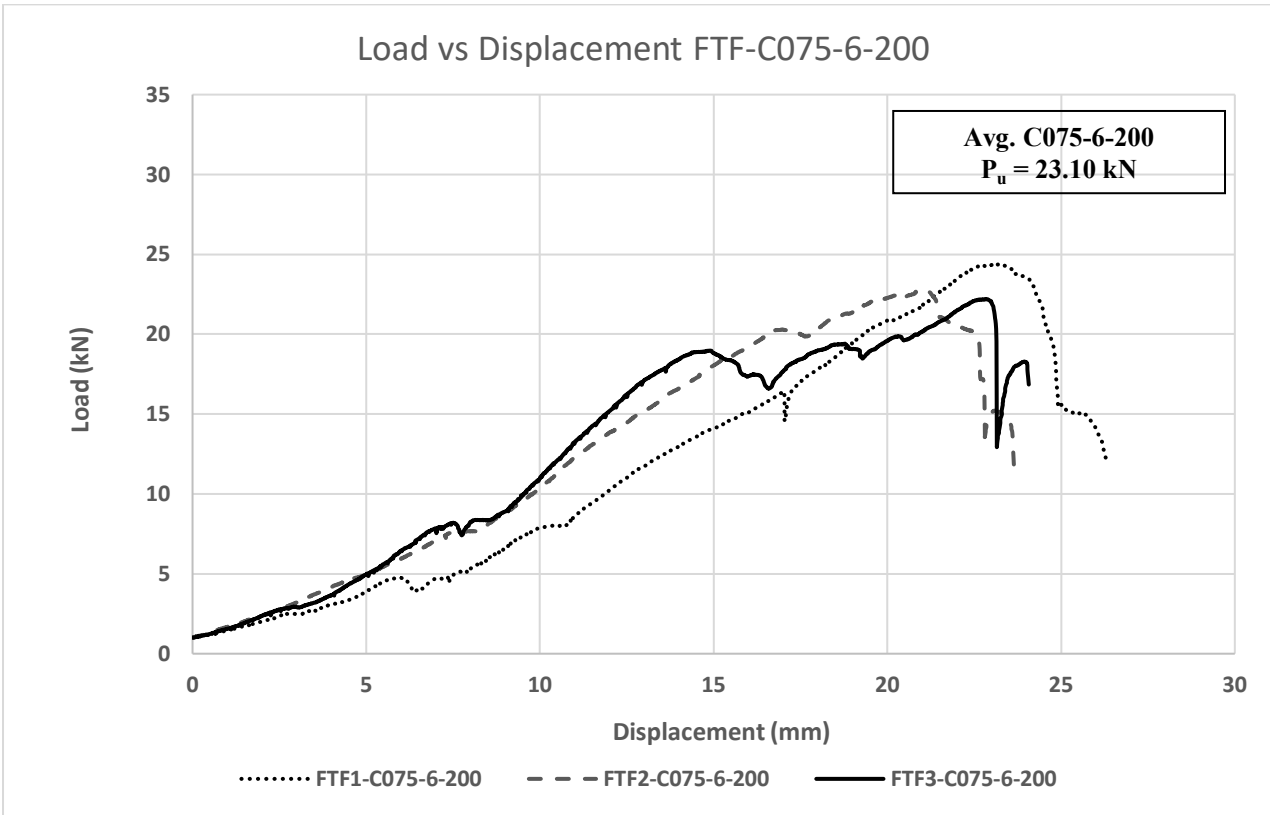

(b)

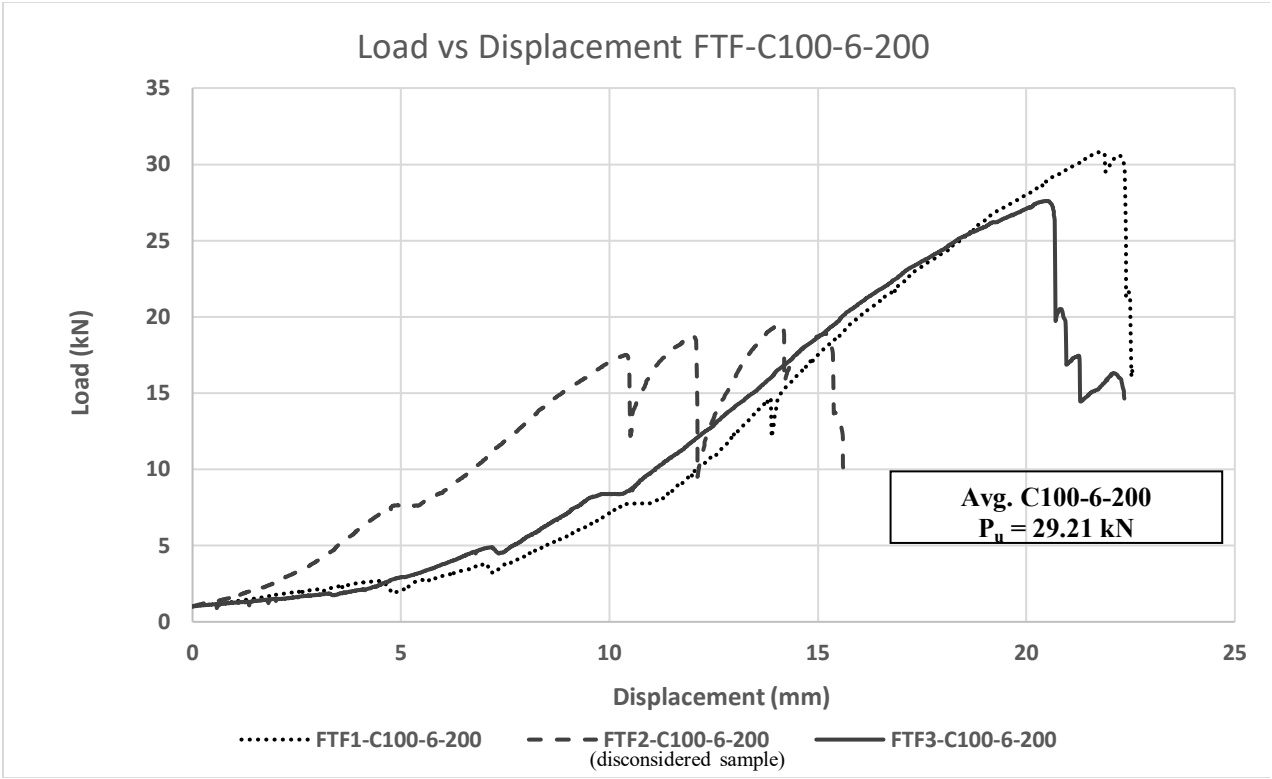

(c)

Fig. 2 *Tensile load against displacement for different thickness of CFS section and number of screws: (a) C075-4-200, (b) C075-6-200, (c) C100-6-200*

The C075-4-200 specimen exhibited early yielding with limited ductility, reflecting its thinner section and fewer fasteners. In contrast, the C100-6-200 specimen demonstrated a longer displacement range and higher peak load, indicating improved ductility and load resistance. As screw number and flange thickness increase, displacement prior to failure becomes more gradual, allowing energy dissipation through deformation rather than abrupt rupture. These behavioral patterns suggest that appropriate connection detailing can enhance both strength and ductility of FTFF connections.

3.2 Analysis of Experimental vs. Analytical Results

Three specimen types were examined with constant sleeve length of 200 mm for samples C075-4-200 (0.75 mm thickness, 4 screws), C075-6-200 (0.75 mm thickness, 6 screws), and C100-6-200 (1.00 mm thickness, 6 screws). A comparison was made between the experimental and analytical predictions from Eurocode 3 for shear and bearing resistances. In general, the $Avg.P_u$ were lower than analytical design resistance values. Based on the calculations, the bearing resistance was 2.27 kN (for 0.75 mm thickness) and 3.82 kN (for 1.00 mm thickness) per hole, and the shear resistance was 5.71 kN per screw. Table 4 presents a comparison of the normalized ratio between experimental tensile loads and analytical design resistances calculated according to Eurocode 3 provisions.

Table 4 *Summary of the result design resistance for laboratory test and analytical.*

Spec. ID	Design Resistance(kN)	Thickness (mm)	Sleeve Length (mm)	Screws	$(N_{exp,}P_u)$ (kN)	$(F_{v,Rd})$ (kN)		$(F_{b,Rd})$ (kN)	
						Shear res.	Ratio	Bearing res.	Ratio
C075-4-200	$F_{b,Rd,0.75}$ = 2.27/hole	0.75		4	15.20	22.84	0.54	9.08	1.67
C075-6-200	$F_{b,Rd,1.00}$ = 3.82/hole	0.75	200	6	23.10	34.26	0.67	13.62	1.39
C100-6-200	$F_{v,Rd}$ = 5.71/screw	1.00		6	29.21	34.26	0.85	22.92	1.27

For specimen C075-4-200, the experimental load of 15.20 kN produced a bearing resistance ratio of 1.67 and a shear resistance ratio of 0.54. This indicates that bearing resistance was fully mobilized and exceeded the EC3 design prediction, while a substantial reserve remained in shear capacity. Increasing the number of screws to six in specimen C075-6-200 resulted in an experimental load of 23.10 kN, with bearing and shear ratios of 1.39 and 0.67, respectively. This shear improvement reflects enhanced load sharing and increased bearing resistance due to the additional fasteners, although shear utilization remained well below its design limit.

The thicker specimen C100-6-200 achieved the highest experimental load of 29.21 kN, corresponding to bearing and shear ratios of 1.27 and 0.85, respectively. Although the bearing ratio decreased slightly compared to thinner specimens, it remained above unity, confirming that bearing deformation continued to govern the connection response. The comparison between specimens C075-6-200 and C100-6-200 shows that the thicker specimen achieved higher shear resistance ratios, coinciding with the improvement in shear capacity measured during laboratory testing.

Overall, the consistently high bearing resistance ratios across all specimens confirm that bearing deformation governs the critical limit state of FTFF connections. In contrast, the relatively narrow range of shear resistance ratios (0.54 to 0.85) indicates that variations in material thickness and screw quantity on shear capacity utilization. The discrepancies between experimental and analytical results can be attributed to factors such as geometric imperfections, hole misalignment, non-uniform load distribution within screw groups, and localized yielding effects that are not fully captured from the design equations.

3.3 Comparative Performance

The comparative performance of the FTFF connections configuration demonstrates that both material thickness and screw quantity influence shear and bearing capacities. Specimens C075-6-200 exhibited a higher experimental tensile load compared configurations with fewer fasteners, implying that an increased number of screws can partially reduce the bearing resistance ratio due to the load distribution. Similar behaviour has been reported in previous experimental studies, where an increase in screw number enhanced overall tensile capacity but reduced the effectiveness of individual fasteners due to non-uniform load distribution and group interaction effects [7].

Experimental results showed that increasing CFS thickness from 0.75 mm to 1.00 mm at similar number of screws led to improvements in $Avg.P_u$ up to 26 %. The thicker specimen C100-6-200 exhibited the highest tensile capacity and increased the bearing resistance, confirming that thickness enhancement directly improves resistance to hole elongation and localized plate yielding, and optimizes the design of the bearing resistance ratio when it approaches unity.

Across all specimens, bearing resistance ratios approached or exceeded unity, while shear resistance ratios remained well below unity, confirming that both shear and bearing govern the tensile behaviour of FTFF connections. This observation is consistent with experimental findings reported in the literature, where bearing failure was identified as the dominant limit state in cold-formed steel screw connections subjected to axial tension, and fastener shear capacity was found to be largely underutilized [7,8,9]. The results further indicate that increasing screw quantity alone does not proportionally increase connection capacity, as interaction effects limit the contribution of additional fasteners. But, prior studies have also shown that excessive fastener numbers may reduce per-screw efficiency and, in some cases, negatively affect shear performance due to over-constraint and uneven load transfer [7,8].

Overall, the comparative analysis confirms that optimal FTFF connection performance is achieved through a balanced design approach, prioritizing the enhancement of bearing and shear resistances through the appropriate configuration of material thickness and the number of fasteners applied to improve the connection detailing. These findings are consistent with previous experimental evidence emphasizing the importance of geometry and thickness over fastener quantity in achieving robust and predictable cold-formed steel connection behaviour [7,9]. It is important for design strategies to consider the appropriate number of screws and plate thickness to achieve an optimized design solution, particularly when both ratios approach unity without compromising the applied forces acting on the connection.

3.4 Failure Modes

The primary failures observed were shear failure (Figure 3a) and bearing failure (Figure 3b). In most cases, the screws exhibited noticeable tilting at the end of testing, while screw fracture did not occur. The other failure mechanism was identified as bearing failure, wherein the applied load induces localized plastic deformation around the screw hole, resulting in measurable elongation and ovalization of the connected plates.

This mode of failure is governed by compressive stresses that exceed the bearing capacity of the material, and is particularly critical in thin-walled CFS members, where stress concentrations form rapidly due to the reduced thickness and limited confinement at the screw interface.

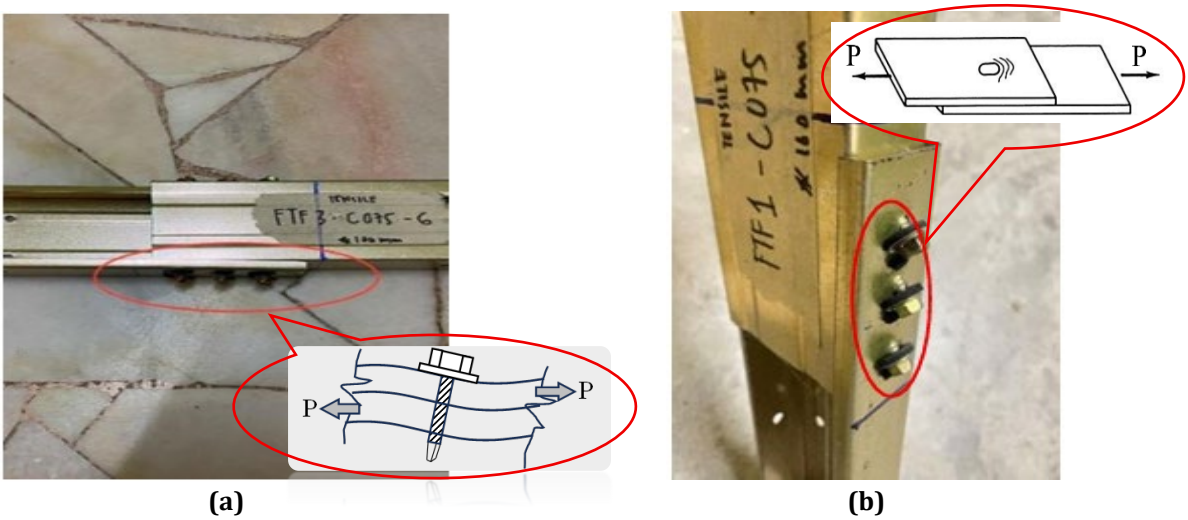

Fig. 3 *Failure mode of failure observed in the tested samples: (a) shear failure; and (b) bearing failure*

Shear failure mode happens when the applied tensile force exceeds the load-carrying capacity of the screws, leading to screw rupture, slippage, or pull-out from the connected plates. The failure was marked by elongation of the holes and tearing along the screw line. Similar mechanisms have been documented by Alif et al. [8], who reported that screw slippage and pull-out reduce the overall connection efficiency and compromise structural reliability.

Plate bearing deformation was observed in the form of screw-hole ovalization accompanied by localized distortion of the connected steel surfaces. This failure mode was predominant in thicker specimens, where the material exhibited sufficient resistance against immediate rupture and instead underwent progressive deformation under increasing applied load. The extent of bearing deformation was strongly influenced by plate thickness, screw diameter, and edge distance, with thinner plates and shorter end distances demonstrating greater susceptibility to this failure mechanism. Similar deformation patterns have been reported in previous studies, including Alif et al. [9], who noted that bearing failure can provide a degree of ductility by allowing gradual load redistribution prior to ultimate failure.

The sleeve connection also contributed to stress redistribution, in some cases delaying but not preventing the onset of bearing failure. The observed deformation characteristics suggest a combination of local yielding, non-uniform load transfer, and group screw interaction effects. These behaviours are consistent with findings reported in the literature. LaBoube and Sokol [4] observed that increasing the number of screws enhances overall load sharing, although the effectiveness of individual fasteners may be reduced due to interaction effects. Similarly, Roy et al. [3] emphasized that connection geometry and fastener spacing play a critical role in governing dominant failure modes.

A detailed understanding of these failure mechanisms is therefore essential for the development of improved FTFF connection designs with enhanced robustness against practical construction imperfections, such as misalignment and fabrication-induced inconsistencies.

4. Conclusion

This study investigates the structural behaviour of face-to-face flange (FTFF) sleeve connections in cold-formed steel (CFS) C-sections, with particular emphasis on bearing and shear resistance mechanisms. Analytical design resistances were evaluated in accordance with Eurocode 3 (EC3) and compared against experimental results obtained from laboratory testing of 9 specimens with varying flange thicknesses, sleeve lap lengths, and screw quantities. The experimental results demonstrate that bearing resistance governs the critical limit state of FTFF connections. Bearing resistance ratios consistently exceeded unity, ranging from 1.27 to 1.67. Bearing deformation, characterized by hole elongation and localized plate yielding, was observed and dominated the failure modes. In contrast, shear resistance ratios remained below unity, ranging from 0.54 to 0.85. This also indicates that shear capacity also governed the performance depending on the number of screws used in the connection configurations. Increasing material thickness and screw quantity improved overall connection capacity primarily. It was further observed that the discrepancies between experimental and analytical predictions may result from additional factors, including geometric imperfections, hole misalignment, non-uniform load distribution among fastener groups, and localized yielding effects that were potentially not fully considered in the design calculations. Future research should extend this work by incorporating numerical

modelling and parametric studies to further investigate the influence of connection geometry and optimize the configuration of fasteners and plate thickness for an optimal design solution.

Acknowledgement

This research was supported by Universiti Tun Hussein Onn Malaysia and the UTHM Publisher's Office under the Publication Fund E15216. The authors thank the FKAAB staff and laboratory technicians for their assistance.

Conflict of Interest

The author declares no conflict of interest.

Author Contribution

The authors confirm contribution to the paper as follows: ***study conception and design:*** *Siti Nur Aishah, Muhammad Alif Irwan & Ahmad Fahmy;* ***data collection:*** *Siti Nur Aishah;* ***analysis and interpretation of results:*** *Siti Nur Aishah, Muhammad Alif Irwan & Ahmad Fahmy;* ***draft manuscript preparation:*** *Siti Nur Aishah, Muhammad Alif Irwan;* ***supervision & review***: *Ahmad Fahmy. All authors reviewed the results and approved the final version of the manuscript.*

References

[1] Fan S, Chen M, Li S, Ding Z, Shu G and Zheng B 2019 Stainless steel lipped C-section beams: numerical modelling and development of design rules J. Constr. Steel Res. 152 29–41.

[2] Wu, H., Sui, L., Liu, X., Liang, S., & Zhou, T. (2023). Shear-slip constitutive model of screw-fastened connections and application in numerical analysis of built-up back-to-back cold-formed steel columns. Thin-Walled Structures, 186, 110710.

[3] Roy, K., Lau, H. H., Ting, T. C. H., Masood, R., Kumar, A., & Lim, J. B. P. (2019). Experiments and finite element modelling of screw pattern of self-drilling screw connections for high strength cold-formed steel. Thin-Walled Structures, 145, 106393.

[4] LaBoube, R. A., & Sokol, M. A. (2002). Behavior of screw connections in residential construction. Journal of Structural Engineering, 128(1), 115–118.

[5] European Committee for Standardization. (2006). EN 1993-1-3: Eurocode 3: Design of steel structures - Part 1-3: General rules - Supplementary rules for cold-formed members and sheeting. Brussels: CEN.

[6] Young, B., & Chen, J. (2008). Design of cold-formed steel bolted connections. Engineering Structures, 30(7), 2001–2009.

[7] Alif, I. R. M., Kamarudin, A. F., Hakim, S. J. S., Zuki, S. S. M., Faisal, A., & Dtauwel, M. (2025). Technical Specification of Extension-Connection for Axial Tension C-Section Cold-Formed Steel (CFS). *International Journal of Integrated Engineering*, *17*(3). https://doi.org/10.30880/ijie.2025.17.03.028

[8] Muhammad Alif, I. R., Kamarudin, A.F., Seyed Hakim, S.J., Musa, M.K., Hamid, S. and Rathomy Romeli, M.A. (2025). Tensile Resistance of Face-to-Face (F2F) Flange Connection of Cold-Formed Steel (CFS) Channel. IOP Conf. Series: Earth and Environmental Science, 1453. (pp. 1-9).

[9] Alif, I. R. M., Kamarudin, A. F., Hakim, S. J. S., Musa, M. K., Hamid, S., Mohammadhasani, M., & Romeli, M. a. R. (2024). Investigation of tensile test on Back-to-Back web connection of Cold-Formed Steel C-Section. In Lecture notes in civil engineering (pp. 343–351). https://doi.org/10.1007/978-981-97-0751-5_34

[10] Hancock, G. J., & Pham, C. H. (2009). Advances in the design of cold-formed steel structures. Thin-Walled Structures, 47(12), 1431–1437.

[11] Huynh, M. T., Pham, C. H., & Hancock, G. J. (2020). Design of screwed connections in cold-formed steels in shear. Thin-Walled Structures, 154, 106817. https://doi.org/10.1016/j.tws.2020.106817